CFD Prediction of Cooling Tower Drift

Prepared by

Robert N. Meroney, Emeritus Professor

Wind Engineering and Fluids Laboratory
Civil Engineering Department
Colorado State University
Fort Collins, CO 80525

October 25, 2004
Revised August 5, 2005
Final Revision February 28, 2006

ABSTRACT:

Drift of small water droplets from mechanical and natural draft cooling tower installations can contain water treatment chemicals such that contact with plants, building surfaces and human activity can be hazardous. Prediction of drift deposition is generally provided by analytic models such as the US Environmental Protection Agency approved ISCST3 (Industrial Source Complex Short Term Version 3) or SACTI (Seasonal-Annual Cooling Tower Impact) codes; however, these codes are less suitable when cooling towers are located midst taller structures and buildings. A computational fluid dynamics code including Lagrangian prediction of the gravity driven but stochastic trajectory descent of droplets is considered and compared to data from the 1977 Chalk Point Dye Tracer Experiment. The CFD (computational fluid dynamics) program predicts plume rise, surface concentrations, plume centerline concentrations and surface drift deposition within the bounds of field experimental accuracy.

KEYWORDS:

Drift, Deposition, Cooling Tower, Computational Fluid Dynamics

1.0 INTRODUCTION

Mechanical and natural draft cooling towers are routinely used to condition air and water for power plants and air conditioning systems. Water droplets become entrained in the air stream as it passes through the tower. When a small amount of circulating water in a cooling tower is entrained and carried aloft by the air stream in the form of droplets, which vary from a few to several thousand microns in diameter, the droplets are referred to as drift. While eliminators strip most of this water from the discharge stream a certain amount discharges from the tower as drift. The rate of drift loss is a function of tower configuration, eliminator design, airflow rate through the tower and water loading. Because such drift contains the minerals of the makeup water and often contains water treatment chemicals, contact of these chemicals with plants, building surfaces and human activity can be hazardous (U.S. EPA, 1984, 1989).

Cooling tower drift includes larger droplets, which fall out of the often-visible fog plume due to the effect of the earth's gravitational field. The rate of descent of the fluid droplets depends upon a balance between the aerodynamic drag force and the gravitational force exerted by the earth on the individual droplet. Sedimentation of such droplets downwind of the cooling towers may result in an increase in ground level concentrations of cooling tower water treatment chemicals. The ground can then retain the chemicals by processes such as impaction and absorption. The transport and dispersion of gases and fine aerosols from the cooling tower exits can be predicted by analytic programs (such as the Industrial Source Complex (ISC3) or the Seasonal/Annual Cooling Tower Impact (SACTI) models) or when significant building interactions are present by physical modeling in environmental wind tunnels. (See Sections 2.1.2 and 2.1.3 for references)

Analytic models such as the ISC3 group include plume rise formulae and adjustments for building downwash, buoyant/dense plume behavior, gravitational settling and wet/dry deposition. These formulae include corrections for building downwash by Huber & Snyder (1982) or Scire & Schulman (1980) based on physical modeling measurements in environmental wind tunnels. The corrections for gravitational settling are calculated from estimates of fall velocity of individual droplets based on physical modeling measurements of drag coefficients for small particles in laboratory facilities. SACTI and some CFD codes also include thermodynamic effects due to phase changes (condensation and evaporation) which can affect plume and drift behavior. Unfortunately, neither of these analytical approaches includes the influence of nearby large buildings on the flow fields, which affect the local building downwash and cooling tower drift. Although the background flow fields and gaseous plume motions can be accurately simulated by physical modeling in environmental wind tunnels at moderate velocities, the correct scaling of droplet and particle drift requires that the simulations be run at extremely low facility velocities, which then distorts the model flow fields (Kennedy and Fordyce, 1974; Jain and Kennedy, 1978). A third approach to estimate drift and droplet deposition which includes the effects of ambient winds, building wakes, exhaust jets and

surrounding buildings and terrain is that of computational fluid dynamics (CFD), i.e. solving the relevant equations of motion by numerical means. This method is primarily limited by computational resources and the accuracy of turbulent models (McAlpine and Ruby, 2004).

This paper discusses the status of computational and hybrid modeling of wind engineering situations in Sections 1.1 and 1.2. Then it reviews existing analytic methods to predict drift in Section 2.1, considers the sensitivity of input conditions during drift predictions in Section 2.2, and examines the methodology used in a typical commercial code, FLUENT, to predict drift in Section 2.3. Section 3.0 compares CFD calculations of drift during the 1977 Chalk Point cooling tower experiments to observations and analytic predictions. Section 4.0 summarizes the results of these considerations and calculations.

1.1 Computational Modeling

Numerical modeling, despite its many limitations associated with grid resolution, choice of turbulence model, or assignment of boundary conditions is not intrinsically limited by similitude or scale constraints. Thus, in principle, it should be possible to numerically simulate all aspects of plume transport, dispersion, and/or drift. In addition it should be possible to examine all interactions of plume properties individually, sequentially and combined to evaluate nonlinear effects (Murakami, 1999; Stathopoulos, 1999). It is this tremendous potential that has led wind engineering practitioners to more frequently present results of such numerical studies in professional and trade journals and promotional materials. Realistically, however, the choice of domain resolution, turbulence models, and boundary conditions constrain predictions.

Hence, continued verification and validation is required at almost every level of CFD prediction (Castro and Graham, 1999; Castro, 2003; Slater, 2004).[1] Various criteria for measuring agreement between predictions and full or model-scale measurements are available including scatter diagrams, classical ANOVA (Analysis of Variance), pattern comparison tests and weighted average fractional bias plots (Shin et al., 1989, 1991). Several organizations have established committees and groups to focus on the quality of and trust in CFD applied to practical applications (e.g. QNET-CFD, 2004; NPARC Alliance, 2004; ERCOFTAC, 2000; AIAA, 1998).

---

[1] *Verification* is defined as the process of determining that a model implementation accurately represents the developer's conceptual description of the model and the solution to the model. Or: Procedure to ensure that the program solves the equations correctly. *Validation* is defined as the process of determining the degree to which a model is an accurate representation of the real world from the perspective of the intended uses of the model. Or:

1.2 Hybrid Modeling

A "hybrid" model is one that results from the union of concepts or results from two unrelated methodologies (eg. experimental and numerical). Hangan (2004) suggested one call the hybrid approach, the C-FD-E concept. The C-FD-E concept considers the interplay between computational fluid dynamics (CFD) and experimental fluid dynamics (EFD). Hangan argues that the two tools have to play complementary rather than opposed roles in the further development of fluid dynamics. There are several reasons why hybrid or joint fluid/computational modeling should be useful for evaluating the validity of dispersion models and even directly predicting the behavior of dispersion during diffusion incidents: theoretical, dispersion comparability, controlled conditions and expense. The very use of the word "hybrid" implies a combination of initially unrelated concepts of heterogeneous origin that results in an offspring that has hopefully the best qualities of both parents. Indeed, such crossbreeding often results in 'hybrid vigor' that has even better and stronger characteristics than either parent. For example,

- Both methods permit the individual control of many variables which permits the analyst to isolate driving or dominant transport mechanisms,
- Fluid modeling can provide data in situations where the actual physical mixing mechanisms are vague, confused or obscured by other phenomena,
- Computational modeling can provide data at greater spatial resolution than is practicable during fluid modeling due to instrumentation, time or cost limitations,
- Dispersion in fluid modeling situations incorporates mixing at all time scales, whereas time dependent solutions in CFD often require the dedication of massive computational resources, and
- Computational modeling can be employed to explore further into the parametric space of a problem.

When used together the analyst is able to confidently assess model reliability, model generality, and model robustness. Indeed engineering groups are often reluctant to make critical design decisions based solely on CFD, instead acquiring similar data from independent sources, such as wind tunnel testing that mitigates the perceived risks due to feared deficiencies in CFD data. Viegas remarked during the 1993 NATO Advanced Study Institute on Wind Climates in Cities that "numerical and experimental methods are complementary, the ideal situation being that both of them are carried out in parallel." (Cermak et al., 1995)

2.0 ANALYTIC AND COMPUTATIONAL PREDICTION OF COOLING TOWER DRIFT

Estimation of the impact of cooling tower drift on downwind deposition of droplet born toxins in the presence of buildings can be difficult. Initial interest in drift was associated with dispersion of radioactive particles from nuclear accidents or nuclear power plant sites (Pasquill, 1962; Van der Hoven, 1968). Later the impact of accumulated salts on downwind vegetation associated with large ocean-side fossil and nuclear power plants using salt-water or

---

Procedure to test the extent to which the model accurately represents reality.

brackish water in natural and mechanical draft cooling towers drove investigations into drift behavior (ASME, 1975). A few field studies performed between 1965 and1984 examined cooling tower plume rise, visibility, and downwind concentrations. Unfortunately, only a couple of these actually measured deposition rates downwind.

2.1 Analytic Models

Despite limited field data, concern about drift and deposition led to more than a dozen separate analytic models to predict downwind ground-level concentrations and deposition rates. Chen (1977) and Chen and Hanna (1978) compared ten drift deposition models using a set of standard input conditions for a natural draft cooling tower. They concluded most of the models agree within a factor of three; however, when all ten models are compared, the predicted maximum drift deposition differs by two orders of magnitude, and the downwind locations of the maximum differ by one order of magnitude. These comparisons occurred before improved sets of field data from the Chalk Point Dye Tracer Experiments were available after 1977.

Policastro et.al. (1978) compared most of the same drift deposition models to the new Chalk Point experimental data. They concluded, "None of the existing models performed well." The authors observed that even for this "best available" data the statistical significance of the data may be questionable considering only 10 to 50 droplets were typically obtained on the sensitive measurement papers over a four-hour period. Policastro et al. (1981a, 1981b) developed the SACTI model specifically to improve drift prediction, yet they concluded for a model to predict within a factor of three of measured data can be considered successful prediction. (Success within a factor of three means the prediction is within the range encompassed by one-third and three times the measured value, but samples where either the measured value is zero or the model prediction is zero are not counted.)

Drift predictions are also quite sensitive to initial conditions. In order to determine how the variations in updraft air speed, temperatures, and drift mass emission droplet spectra would affect drift transport modeling results, Webb et al. (1978) performed a sensitivity study using input data gathered during the Chalk Point Cooling Power Project in 1976. They inserted these variations into the ESC/Schrecker drift model (still considered a model nearly on par with the SACTI model). The standard deviations of test averages for tower exhaust velocity, tower updraft air temperature, and emission rates varied by 13, 4.5, and 42 % respectively. Drift mass emission varied by factors from 24 to 3 for droplet sizes at 1000 and 50 μm, respectively. Consequently, predicted deposition rates varied by factors of 60, 15, 8 and 3 at 300, 500, 1,000 and 10,000 m, respectively. They concluded variations in the drift emission droplet spectrum have the greatest effect on model calculations of downwind mineral mass deposition.

A review of available drift models suggest that currently the most frequently used for short range transport are the K.S. Rao modifications to the EPA Point, Area Line Source Algorithm (PAL2.1), the EPA Industrial Source

Complex Short Distance 3 (ISCST3) model, and the Argonne National Laboratory Seasonal/Annual Cooling Tower Impact (SACTI) model. These are considered in detail below.

2.1.1 PAL2.1 Model: This model was undertaken to develop concentration algorithms for the EPA Pollution Episodic Model (PEM) in the early 1980s (Petersen and Rumsey, 1987). The analytical plume model predicts atmospheric transport, diffusion, deposition, and first-order chemical transformation of gaseous and particulate pollutants. It treats gravitational settling and dry deposition from elevated sources by solving the equations of motion based on gradient transfer or K-theory (Rao, 1981, 1983). The model's strength is its simplicity and ease of use. Unfortunately, its greatest disadvantages are also its simplicity since it does not adjust for complex building environments where separation, reattachment and recirculation of the flow field can occur. It is not a true ballistic trajectory model; hence, it is less likely to predict the behavior of large droplets near (within 1-2 km) of the source well. This model is also described briefly by Hanna, Briggs and Hosker (1982) in their well-known *Handbook of Atmospheric Diffusion.* This model has not been used extensively recently, but it is included here due to its historical significance, and its analytic rigor.

2.1.2 ISCST3 Model: The most widely used air quality model is the U.S. Environmental Protection Agency's Industrial Source Complex Short Term Model 3 (ISCST3). This model is used to address the air quality impacts from stationary sources to demonstrate compliance to permitting regulations. While the model is useful for estimating pollutant concentrations beyond the zone of building wakes it is not intended for analysis within a recirculation zone nor can it account for air movement deflections and turbulence caused by obstructions downwind from the source complex.

The ISCST3 model provides options to model emissions from a wide range of sources that might be present at a typical industrial source complex. The basis of the model is the straight-line, steady-state Gaussian plume equation, which is used with some modifications to model simple point source emissions from stacks, emissions that experience the effect of aerodynamic downwash due to nearby buildings, isolated vents, multiple vents, etc. (U.S. EPA, 1995b). Emissions are categorized into four types, i.e., point sources, volume sources, area sources, and open pit sources. The model accepts hourly meteorological data records to define the conditions for plume rise, transport, diffusion and deposition. Plume rise caused by momentum or buoyant forces are accounted for by adjusting the source height and plume trajectory. Thermodynamic effects on plume behavior, specifically latent heat effects due to condensation or evaporation of water vapor or drifting particles are not included. Seasonal or annual concentrations are calculated by weighting downwind results for time dependent variations in source strength, wind fields, wind directions and climatic stability.

Particles (or droplets) included with the emissions are brought to the surface through the combined processes of turbulent diffusion and gravitational settling. Once near the surface, they may be removed from the atmosphere and

deposited on the surface. The removal is modeled in terms of deposition velocity (v_d), by assuming the deposition flux of material to the surface is equal to the product $v_d\chi_d$, where χ_d is the airborne concentration just above the surface. Such deposition reduces the concentration of particulates within the plume, and thereby alters the vertical distribution of the remaining particulates. A corrected source-depletion model developed by Horst (1983) is used to obtain a vertical term that incorporates both the gravitational settling of the plume and the removal of plume mass at the surface. These effects are incorporated as modifications to the Gaussian plume equation. Gravitational settling is assumed to result in a "tilted plume", so the effective plume height of the release constantly decreases at a rate proportional to droplet settling velocity, v_g. Then local ground level concentrations are adjusted by a "source depletion factor" that can be considered a ratio of the current mass emission rate to the original mass emission rate, and the remaining source mass is also redistributed in the vertical to account for the mass adjustment.

The adjustment factors depend on the size and density of the particles being modeled because they affect the total deposition velocity; hence, for a given source of particulates, ISCST3 allows multiple particle-size categories to be defined. The final deposition at the wall then becomes the sum of the terms for each particle-size category, weighted by the respective mass-fractions.[2]

2.1.3 SACTI Model: Staff at the Argonne National Laboratory working for the Electric Power Research Institute developed this model to predict plume and drift behavior from multiple tower and cell configurations of natural and mechanical draft cooling towers (Policastro et al., 1981a, 1981b). The SACTI Model incorporates a number of significant improvements over previous analytic models. These include i) use of an advanced integral model for cooling tower plume trajectory and dispersion (Schatzmann and Policastro, 1984), ii) incorporation of improved droplet evaporation models which include adjustments for ambient temperatures, humidity and the effects of dissolved solids,[3] iii) the choice of up to five "breakaway models" for when the droplets leave the cooling tower plume and enters ambient air, and iv) the use of ballistic trajectory calculations to determine behavior of individual droplets as they change droplet diameter and move from within the plume to ambient air with associated changes in air speed and drag. The model does include empirical corrections for the effects of tower downwash on the gross plume motions through a modification of the entrainment function; however, it does not include corrections for the influence of upwind or downwind buildings or terrain.

The behavior of the single plume SACTI Model was validated against the Chalk Point Dye Tracer Study (Policastro et al., 1978b, 1981a). The behavior of the multiple plumes SACTI Model was validated against the multiple unit mechanical draft cooling towers at Pittsburgh CA (Policastro et al., 1981b). They concluded a model that could

[2] Another EPA promoted program which includes deposition based on droplet size and gravitational settling is the model CALPUFF (U.S. EPA, 2003). This model is primarily recommended for long range transport (distances > 50 km), but includes similar physics for calculating particle movement and deposition as ISCST-3.
[3] SACTI is the only analytic model which properly accounts for phase changes and latent heat effects.

predict deposition within factors of 3 should be considered sufficiently accurate given the uncertainties in meteorology, cooling tower performance, and model assumptions. Comparisons were presented for sodium deposition flux, drop number flux, average diameter, and liquid mass deposition flux.

The Chalk Point facility included two large natural draft cooling towers located in flat tide-water terrain on the Chesapeake Bay, MD. Data were limited to moderate-to-large wind speed, high ambient relative humidity, and strongly stable ambient stratification. Hence, only a minimal effect of droplet evaporation and ambient turbulence effects were examined. Deposition of Rhodamine-WT fluorescent dye tracer was measured only at 500 and 1000 m downwind of the cooling tower. The fallout of larger droplet diameters will dominate deposition at these short distances. For the Chalk Point comparisons they concluded that, given the "correct" choice of breakaway criterion, agreement occurred with only one failure over the entire measured data set, and they asserted the SACTI model was as good as or better than other drift models.

The Pittsburgh facility consisted of seven oil-fired units. Units 1-6 employed once-through cooling, while Unit 7 is cooled by two 13-cell rectangular mechanical draft cooling towers located 0.5 km from the unit. The towers were stated by the manufacturers to have a guaranteed drift rate of 0.004%, but leaks around the cooling tower drift eliminators allowed significantly higher drift emissions in some cases. Data were sampled along five arcs located between 120 to 750 m downwind of Tower Unit 7-1 and between 250 to 1000 m downwind of Tower Unit 7-2. Downwind deposition measurements were often coordinated with simultaneous source measurements. Eight field surveys were conducted during June 1978. For model comparisons a single-composite drift droplet spectrum was used independent of test date. For the Pittsburgh comparisons the authors concluded that the SACTI model predicted deposition within a factor of 3, 50% of the time.

2.1.4 Model Limitations: These analytic models have assumptions which limit their application to near field transport and diffusion. They are:

- Stack emission downwash adjustment presumes the source building and its stack is not in the recirculation region of other buildings,
- The effect of streamline deflection on plume trajectories is not considered,
- The effect of the velocity deficit in the wake on plume rise is neglected;
- There is no accounting for plume material captured by the near wake on far wake concentrations,
- Stack plume height adjustment algorithms presume the building is a simple rectangular form with characteristic height, width and depth,
- Plume concentrations are not reliably predicted within the immediate recirculation region of the building wake, and

- The model does not account for the effect of any upwind or downwind buildings on plume trajectory or enhanced dispersion.

In addition the PAL 2.1 and ISCST3 models are further constrained because:

- Gravitational settling algorithms used assume relevant particle sizes are small (< 0.1 mm); hence, the model does not predict the behavior of large particles,
- Thermodynamic effects of condensation and evaporation on plume and drift behavior are not considered, and
- The programs do not adjust for the effect of the interaction of large nearby source jets (like multiple cooling tower units on a mechanical draft cooling tower) on plume rise and turbulent mixing.

Some of these limitations have been addressed in the development of the ISC-PRIME and AERMOD-PRIME models proposed to replace the ISC-3 series (Schulman, et al., 2000; Petersen, 2004); however, although PRIME can be used with more than one building close to the source stacks, it cannot be used to compute the plume path through or affected by the building cavities for another building or group of buildings at a distance downwind from the initial industrial source complex (Ruby and McAlpine, 2004).

2.2 Droplet Particle Distributions at Cooling Tower Exit

Cooling tower drift consists of droplets from the cooling water stream, which are entrained out of the tower in the exhaust gas flow. In order to minimize drift emissions, modern cooling towers commonly employ drift eliminator systems. The magnitude of the drift loss is influenced by the number and size of droplets produced within the cooling tower. These are in turn determined by the fill design, air and water patterns (counter flow, cross flow, fan assisted, induced draft, etc.), type of drift eliminator installed, etc. (U.S. EPA, 1995; Moore et al., 1978).

To reduce the drift from cooling towers, drift eliminators are usually incorporated into the tower design to remove as many droplets as practical from the air stream before exiting the tower. The drift eliminators rely on inertial separation caused by exhaust flow direction changes while passing through the eliminators. Types of drift eliminator configurations include herringbone (blade-type), waveform, and cellular (or honeycomb) designs. Drift eliminators are typically rated in terms of the percentage of recirculating cooling water flowing through the system that escapes the tower. Lower efficiency systems are those, which produce values between 0.008 to 0.02 percent, whereas higher efficiency systems claim performance levels of < 0.008 percent. (U.S. EPA, 1989, 1995; Becker and Burdick, 1994)

Many measurement techniques are used to measure droplet distributions. No single method enjoys universal acceptance as the best overall drift measurement technique. In the absence of comprehensive comparative analysis of the various measurement devices, it is difficult to make comparisons of data obtained with different equipment (Golay et. al., 1985). It is also possible that many of the methods used to measure droplet distributions are biased toward smaller particles (ASME, 1975; Chen and Hanna, 1977).

Webb et al. (1978) concluded that predictions of drift deposition were most sensitive to the initial choice of droplet particle distribution at the cooling tower exit. Schrecker (1978) noted that during the Chalk Point experiment some 16 drift-droplet size distributions were measured over the tower's exit plane on different days. The variability of the measured data were large enough that his predictions by analytic models produced deposition rates at distances less than 1 km which varied by factors of 10 and at greater distances by factors of 3.

Quite frequently measured droplet distributions are bimodal with peaks at small and medium or large droplet diameters. It is likely that such distributions are associated with inadequacies in design or subsequent maintenance of drift eliminators. Large droplets of the order of 1000 microns may be generated by i) gaps in the drift eliminators caused by cooling tower structural members, ii) variations in local air velocities due to fan or tower configuration outside the drift eliminator design range, and iii) re-entrainment of collected drift occurring due to water accumulated on structural members, cooling tower fan blades, and the surface of the fan stack. Since these surfaces are downstream of the drift eliminators, the droplet size is determined by the entrainment process and local velocity (PGT, 2003). Indeed, emissions from such sources may comprise most of the mass of the drift emitted by cooling towers. Consequently, the prediction of the size distribution of the drift for a cooling tower can be subject to great uncertainty.

Nonetheless, if deposition predictions are to be made, an informed selection of a "reasonable" droplet distribution is necessary. A review of the literature produced nine sets of data for the cumulative mass fraction distributions of droplets (Lindahl, 2003 [typical Marley MDCT]; Hanna et al., 1978 or 1982 [Chalk Point NDCT (Natural Draft Cooling Tower)]; ERT, 1978 [Hat Creek MDCT (Mechanical Draft Cooling Tower)]; Policastro et al., 1981b [Pittsburgh CA MDCT]; Wilber and Vercauteren, 1986 [Palo Verde MDCT]; Chen and Hanna, 1978 [Idealized normalized distribution]; Chen and Hanna, 1978 [Turkey Point MDCT]; Jallouk et al., 1975 [Oak Ridge National Laboratory MDCT]; and Wilstrom and Ovard, 1973 [Ecodyne MDCT].

The cumulative mass fraction for these cases tended to decrease exponentially with increasing particle diameter; hence, the data were fit to a Rosin-Rammler particle distribution of the form:

$$\text{Cum Mass Fraction} = \exp\left(-(d/d_{mean})^{n}\right),$$

where d_{mean} is the mean particle diameter, and n is known as the shape factor. Comparisons resulted in the following table:

Table 1: Mean Diameter and Shape Factor Parameters in Rosin-Rammler Cumulative Mass Fraction Distributions

Data Set	d_{mean} (mm)	n
Marley MDCT	0.09	1.00
Chalk Point NDCT	0.09	0.65
Turkey Point MDCT	0.07	1.20
Hat Creek MDCT	0.15	0.85
Pittsburgh MDCT	1.00	1.00
Oak Ridge MDCT	0.10	1.00
Palo Verde MDCT	0.45	1.75
Chen & Hanna Idealized	0.30	2.00
Ecodyne MDCT	1.80	0.85

Data seems to fall into two categories with either d_{mean} ~ 0.1mm and n = 1.0 or d_{mean} ~ 1.0 mm and n = 1.0. The second category reflects the presence of a significant number of large particles. In a private communication Policastro (2004) remarked that droplet distributions often had more large droplets than manufacturers like to admit due to end losses, splash and condensation on the cooling tower structure with subsequent re-entrainment.

2.3 CFD Model of Cooling Tower Drift

An alternative approach to estimate drift deposition is to use CFD (Computational fluid Dynamics) to predict both the flow field and the droplet drift patterns in the near vicinity of the cooling towers. Recent improvements in numerical solution algorithms, increases in computational speeds, new turbulence models, and increased storage capacity in computers now make it possible to calculate reasonably large and complicated domains of atmospheric motions in complex urban settings.

There are many general-purpose commercial CFD models that have typically taken tens of thousands of man-hours to develop. These general models often contain features that permit solution of two phase flows, compressible flows, chemical reactions, discrete particle tracking, etc. These full-featured codes include attractive pre-processors to construct grids, specify chemical reaction expressions, and apply initial conditions, processing algorithms that permit segregated or coupled, steady or unsteady state flows and a variety of turbulence models, and post-processors

that display results in a manner that enhance interpretation. Typical packages include CFD2000, CFX-4, CFX-5, CFD Taskflow, FLOW-3D, FLUENT, PHOENICS, STAR-CD, etc. (A list of currently available commercial packages and references can be found at http://www.icemcfd.com/cfd/CFD_codes_c.html).

A number of researchers have used CFD to calculate cooling tower plume behavior. England et al. (1973) used a three-dimensional CFD code to calculate dry and wet cooling tower plume behavior downwind of the Keystone Power Plant in western Pennsylvania. They assumed the Boussinesq approximation for thermal effects, set the along-wind velocity component to a constant, and solved for plume trajectory and plume induced perturbations using a set of linearized vorticity, streamline, energy, and humidity equations. For the dry plume case the single plume height measurement available fell very close to the calculated values, and for the wet plume cases the single plume height measurements available fell within 10 to 25% of the calculated values. Cloud visibility, temperatures, cloud water content, and rain water contours were also calculated, but no comparisons were provided.

Bergstrom et al. (1993) reported the results of a 2-dimensional simulation of the interaction of the flow through an idealized cooling tower with the wind flow over the tower. The porous inlet walls and exhaust fans were modeled as infinitesimal active structures with specified pressure steps and flow velocities. Wind fields were found to substantially increase the inlet flow on the windward side of the tower. Later Derksen et al. (1996) and Bender et al. (1996a and 1996b) reported on a wind tunnel and numerical study on the effects of wind on air intakes and flow rates of a cooling tower. They used wind tunnel results to validate their numerical code before evaluating the effects of protective wind walls to reduce flow asymmetries about the cooling tower.

Finally, Takata et al. (1996) calculated the effects of wind on the visible envelope of moist cooling tower plumes using CFD. Their model solved the momentum, energy and moisture equations for three different size cooling towers using a RNG kappa-epsilon turbulence model on a set of nonuniform hexagonal-mesh three-dimensional grids ranging from 125,000 to 335,000 cells in size. Takata et al. compared their calculated plume dimensions to plumes photographed above equivalent cooling towers whose fan diameters were 1.6, 5.49 and 7.92 m, respectively. Calculated plume length (m), width (m), and volume (m^3) agreed with measured field values within 0 to 17%, 0 to 30%, and 5 to 56%, respectively. No CFD calculations were found in the literature that predicted deposition levels downwind of cooling towers.

Modern computer codes provide wide computational flexibility and several alternatives for multi-phase flow simulations. The nature of CFD models and their structure can be studied in many modern reference books (Anderson, 1995). The movement of cooling tower drift can be calculated via various multi phase mixing models. Eulerian-Lagrangian models calculate the background flow field using conventional RANS or LES solution procedures, and then individual particles are tracked in space using DPM (Discrete Particle Models). Eulerian-Eulerian models treat the droplets as a separate dispersed phase and both the background flow field and the droplet

species are calculated using RANS (Reynolds Averaged Navier Stokes) or LES (Large Eddy Simulation) turbulence models. Sometimes both methods can be used to provide a crosscheck on computational reliability (Fluent 6.1 User's Guide, 2003).

2.3.1 Fluid Modeling: The software solves the three-dimensional Reynolds averaged equations of motion discretized using a control volume approach for flow, pressure, turbulence, and concentration distributions (Fluent 6.1 User's Guide, 2003). The Reynolds stress terms are modeled by one of several turbulence models. Since in this study the behavior of cooling tower drift is emphasized and not flow in bluff-body separation and recirculation zones, the standard kappa-epsilon turbulence model with standard wall functions was considered adequate; however, the RNG or realizable kappa-epsilon models might be more appropriate for cases including shorter mechanical-draft cooling towers and surrounding structures because the standard model is known to over-predict turbulence energy production in strong shear zones. The standard kappa-epsilon turbulence model assumes isotropic turbulence at the sub-grid scale and uses transport equations for the turbulent kinetic energy (κ) and its dissipation rate (ϵ). Ground and wall surfaces were specified as rigid planes with a specified roughness. Inlet (upwind) velocity and turbulence profiles were selected to reproduce field observations.

The conservation equations for momentum, energy and species were solved by using an implicit formulation of the equations, solved in an iterative manner with a segregated protocol (i.e. equations are solved sequentially not simultaneously). Once the flow field, temperature and vapor distributions were determined, the solvers were turned off and the resulting flow and turbulence fields were used to predict particle trajectories as discussed in the next section.

2.3.2 Discrete Phase Modeling: Once a total flow field is defined, the software may be configured to calculate the Lagrangian particle tracks of drift droplets emitted from the cooling tower exhaust nozzles. Particle sizes can be uniform or a specified particle distribution. Particle material can be inert or droplets that undergo evaporation and change in diameter over their lifetime. Particle trajectories can be calculated as simple ballistic trajectories uninfluenced by turbulence, or they can include stochastic dispersion due to the weighted effects of local turbulence and wind speed variations. For the Lagrangian stochastic approach droplets are released from the cooling-tower stack and their movement tracked based on the pre-calculated mean wind field and turbulence properties predicted by the RANS model. The particle positions are obtained by integrating the trajectory equations using the instantaneous fluid velocities ($U_i + u'_i$) along the particle path, where U_i are the mean velocity components and u'_i are the velocity fluctuations related to the local turbulence intensity through a normally distributed random number, which is constant for each "eddy lifetime". Alternatively, the software can be configured to simultaneously calculate fluid motions and particle behavior. This option permits the inclusion of phase change effects on plume rise and droplet size as the particles evaporate or condense during travel; however, inclusion of this option can significantly increase computational time since the calculation requires a full transient solution. Specific solution

details and boundary conditions used in this paper for the flow and DPM model components are summarized in Section 3.2.2: *CFD Simulation of 16 June 1977 Conditions at Chalk Point*.

3.0 VALIDATION OF MODEL DRIFT PREDICTIONS

In principle, it should be possible to numerically simulate all aspects of cooling tower plume dispersion and drift within rural and urban canopies. In addition it should be possible to examine all interactions of plume properties individually, sequentially and combined to evaluate nonlinear effects. Realistically, however, the choice of domain resolution, turbulence models, and boundary conditions constrain predictions. A validation process reveals which situations are modeled with confidence and which configurations produce less reliable predictions.

Riddle et al. (2004) compared FLUENT and ADMS (Atmospheric Dispersion Modeling System: a quasi-Gaussian model) calculations of stack plume dispersion in a typical neutral atmospheric boundary layer. They estimated plume spread and centerline concentration decay using the Lagrangian particle tracking option, and concluded the simulations were satisfactory. Meroney et al. (1999, 2000, 2001, 2002a and 2002b) and Banks et al. (2003) examined the simulation of flow, pressure, concentration and turbulence fields over various obstacles and obstacle arrays using CFD software. Again CFD reproduced wind tunnel experiments quite well. Rather than repeat these types of comparison here, validation will focus on the specific ability of the program to predict the distribution of particle deposition using the DPM methodology. An effort was made to identify suitable field deposition data for cooling tower configurations, but only the Chalk Point Dye Tracer Experiment performed in Maryland in 1977 discussed in Sections 2.1.3 and 2.4.2 was found to provide a simply configured experiment with well-documented surface deposition.

3.1 Particle Trajectory and Fall Velocity Comparisons

Many options in a commercial code are imbedded within the compiled executable program and not immediately available to evaluation by the user; but code verification can be attained through simple virtual experiments that verify performance. One such experiment was performed using a two-dimensional rectangular domain with a uniform velocity cross flow and no turbulence. (In this case the fall velocity algorithms not the mixing characteristics of a turbulent field were of interest.) The tracks of different diameter particles released mid stream in a gravity field were calculated. The particles descend downward at a constant measurable rate (straight line trajectories across domain). This rate is related to the implied drag characteristics and fall velocity of the particle. Particle trajectories were simulated for diameters ranging from 2 mm to 0.001 mm, and in every case the implied fall velocities agreed with those calculated by the equations proposed by Engelmann and summarized by Hanna et al. (1982).

In another virtual experiment simulated gas tracers were released in a uniform cross flow including background turbulence. Isocontours of the resulting downwind concentrations were overlaid over contours produced by analytic predictions for neutral atmosphere plume behavior as calculated by Gaussian plume formulae suggested by Hanna et al. (1982). Plume growth and concentration decay were very similar, well within the error bounds accepted for the analytic formulae.

3.2 Chalk Point Dye Tracer Experiment:

Results from the Chalk Point Dye Tracer Experiment are described in papers and reports by Hanna (1978) and Policastro et al. (1978a, 1981). These experiments are the best single source cooling tower deposition data available. Two natural draft hyperbolic cooling towers are located on the site on a peninsula that extends into the local bay and wet lands. The two towers and the turbine building are located along a east-west line each separated from one-another by about 500 ft. The hyperbolic cooling towers are 400 ft (124 m) tall by 374 ft (114 m) diameter base by 180 ft (54.8 m) diameter exit. (Figure 1)

3.2.1 Field Experiment 16 June 1977 at Chalk Point: Although a number of sodium deposition experiments were performed most results were also affected by simultaneous releases from other nearby stacks and towers as well as wind blown brackish water spray from the bay. But during the evening of 16 June 1977, 30 gallons of 20% Rhodamine WT (fluorescent) dye were added to the cooling tower basin water, and no additional water was added to or drained from the basin during the experiment. Consequently the only loss of dye was through drift loss, and the concentration of dye in the water remained constant for the duration of the experiment. Plant load also remained constant during the experiment. Source measurements reported that drift loss ~0.002%, plume temperature = T_{vp} = 315.3 ^{o}K, ambient temperature = T_{ve} = 295.3 ^{o}K, and exhaust velocity = V_s = 4.5 m/s. Rhodamine WT (fluorescent dye) tagged sodium source strength equaled 1.86 g/sec. Measured cumulative mass fraction and particle number distributions versus particle diameter are plotted in Figures 2 and 3. Measurements were made at night during 93% humidity, so there was negligible droplet evaporation. Predominant winds were from the south at 350^{o}; hence, building and tower wakes did not intersect in the near field. The wind speed profile was in two layers: above 100 m, the wind speed was nearly constant with height, averaging about 8 m/s; below 100 m, the wind speed was nearly linear with height with a mean value of about 5 m/s.

Instruments to measure drift deposition were placed at 5^{o} intervals on 35^{o} arcs at distances of 0.5 and 1.0 km north of the cooling towers. The average deposition of the dye tagged sodium droplets on the 0.5 and 1.0 km arcs was 1080 and 360 kg/km^2-mo, respectively. Drift droplet sizes at the measurement stations had a mass median diameter of 340 and 260 μm on the 0.5 and 1.0 km arcs, respectively. Most of the drop sizes were between 250 and 450 μm on the 0.5 km arc and 200 and 400 μm on the 1.0 km arc. In addition plume centerline heights were observed for the downwind distance range of 50 to 200 m, and Hanna (1978) predicted tower plume centerline trajectories during

the tracer experiment using standard plume rise formulae (Plume Rise = 1.6 $F^{1/3}$ $x^{2/3}$ / u, where F = 2100 m^4/sec^3 and u = 8 m/sec, see Figure 4).

3.2.2 CFD Simulation of 16 June 1977 Conditions at Chalk Point: A CFD simulation was prepared to replicate the Chalk Point results. The intention was to validate the DPM deposition option against field data before using the approach in a more complicated building environment. In summary, the case was selected because:

- Source cooling tower was located in flat unobstructed terrain,
- Source orientation was such that other buildings should not affect plume behavior,
- Source droplet distribution was well documented,
- Measurements of droplet deposition by three different groups all agreed within a reasonable range,
- Plume rise and trajectory are documented,
- Approach wind field and cooling tower exhaust were well documented over the night of deposition measurements, and
- Humidity levels were high which reduced the influence of any droplet evaporation.

On the downside atmospheric conditions were slightly stable, and deposition measurements were made at only two downwind distances.

Calculations for the Chalk Point Cooling Tower simulation were performed on a domain 2000 m long, 1000 m wide and 500 m height using 165,000 tetrahedral cells. The simulated hyperbolic cooling tower was modeled using a cone frustum with a tower height of 124 m, base radius of 40 m, and exit radius of 27.4 m; and plume vertical exhaust speed was set to 4.5 m/sec. Plume buoyancy was included by setting the plume virtual ambient temperature to 295.3^o K, and the virtual exhaust temperature was set to 315.3^o K. Virtual temperatures are used to account for water vapor content and ambient humidity (Hanna, 1978).

For the cooling tower plume simulation considered here, the following conditions were selected:

- Solution domain of typically 2000 m length, 1000 m width and 500 m height. Cooling tower and coordinate origin was centered 500 m downwind of the entrance.
- Tetrahedral grid volumes distributed in size over the domain such that grid increments near buildings and the ground were of the order of 2-4 m with sizes ranging up to 50 m along the top of the domain at 500 m above the ground. Total grid mesh was of the order of 165,000 cells.
- Upwind velocity inlet conditions were set by two separate methods. In Case A upwind inlet profiles were specified to produce a reference velocity of 5 m/sec at a height of 50 m distributed vertically with a power law velocity coefficient of 1.0 up to 100m and with constant velocity of 8 m/sec above 100 m. Inlet turbulent intensity was 10% with characteristic length scales of 50 m. In Case B upwind inlet profiles were produced by a separate CFD virtual wind tunnel calculating over a similar size domain using the same inlet profile, but the outlet profiles of velocity, turbulence kinetic energy and dissipation from the CFD virtual wind tunnel was used subsequently as the inlet profiles for the cooling tower calculations. Temperature inlet was set to 295.3^o K.
- Ground surface roughness height was specified as 0.5 m (~z_o = 0.02 m)
- Domain sides and top were specified as symmetry planes.
- The standard kappa-epsilon turbulence model was specified.

- Velocity exit conditions for the cooling tower were set to 4.5 m/sec with constant turbulent intensity of 10% and length scales of 25 m. Cooling tower exit temperature was set to 315.3^{o} K.
- The SIMPLE algorithm was used to adjust for pressure effects on the flow field.
- All calculations were performed using discretization providing second-order accuracy.
- Steady-state solution results were sought with iterations sufficient to reduce all residuals less than 0.001.
- Given the high humidity conditions experienced during the field experiment, water vapor condensation or evaporation and drift droplet evaporation effects on cooling tower plume dynamics were not considered significant; hence, latent heat effects were not included.

For the cooling tower drift simulation considered here, the following discrete particle model (DPM) conditions were selected:

- Particle material was liquid water.
- Particles were specified to be inert with no evaporation effects.[4]
- (Case 1) Particle size distribution was specified to be a Rosin-Rammler type with:
  d_{mean} = 0.09 mm,
  $d_{minimum}$ = 0.001 mm,
  $d_{maximum}$ = 1.0 mm,
  n (shape factor) = 0.65,
  Source strength of 1.86 g/sec distributed among droplets as noted in Figures 2 and 3.
  10 particle increments over the specified range, and
  Initial particle velocity, V_z = 4.5 m/s.
- Particle trajectories were calculated by the stochastic tracking option with
  Random eddy lifetime option on, and
  Time scale constant = 0.15.
- (Case 2) Deposition was also calculated separately for uniform droplet diameters and individual contributions added to estimate droplet deposition as suggested by Hanna (1978). Droplet mass fractions for each droplet range (11) were assigned per Table 3 from Hanna (1978).
- (Case 3) Finally, deposition was also calculated separately for a modified Rosin-Rammler droplet distribution chosen to replicate the droplet range found in Table 3 from Hanna (1978)
  d_{mean} = 1.0 mm,
  $d_{minimum}$ = 0.15 mm,
  $d_{maximum}$ = 1.4 mm,
  n (shape factor) = 1.0,
  Source strength of 0.4 g/sec (to reflect fact only 21% of sodium source strength falls into this particle range.), and 20 particle increments were used over the specified range.

3.2.3 Results of Chalk Point Validation Exercise: Height of the centerline of the cooling tower plume was determined based on the height of the maximum in the water vapor (gaseous) and temperature profiles downwind of the cooling tower. These calculated points are included on Figure 4 as filled triangles and labeled as CFD Fluent 6.1 data. The calculated points agree very well with the predictions of the Briggs plume rise formulae calculated by Hanna (1978) as well as with the magnitude of the visual observations for plume height recorded during the experiment.

---

[4] Computational runs including evaporative effects produced minimal changes in deposition over the test domain since transport times were short before deposition of particles greater than 0.01 mm occurred; hence, due to the high computational times required for these runs evaporative effects were not included for the comparison runs.

Calculated velocity and turbulence intensity profiles approaching along the domain centerline for Case A are shown in Figures 5 and 6. Note the near constant magnitude 8 m/s velocity values above 100 m and the linear velocity gradient below 100 m with average speeds near 5 m/sec in the upwind boundary layer. But 100 m downwind of the tower the velocity profile shows evidence of the tower wake and the elevated cooling tower plume. Further downwind the velocity profiles show the effects of vertical mixing due to tower wake and plume turbulence. Entrance profiles for Case B were not as satisfactory for they displayed a parabolic profile that reached a maximum at 300 m. Turbulence intensities for both cases increase near the ground to values near 15-20%, which is the correct order of magnitude for near ground turbulence in the atmosphere. At 100 m downwind of the tower enhanced turbulence occurs due to tower wake and plume mixing. Profiles of velocity magnitude for Case A which indicate the wake effects of the cooling tower are displayed on Figure 7 (x = -475, 100, 500, 1000, and 1500 m along centerline and 250 m to side). Figure 7 also includes a clipped section of the isoconcentration surface of constant water vapor mass fraction ~ 0.01 resulting from an assumed release mass fraction of 0.05. Note that the water vapor plume rises and does not mix significantly downward toward the ground over the test domain.

Predictions of water vapor (gaseous) isocontours for Case A in terms of log K factors, (log C^*U_{ref}/Q_{source}), are shown in Figure 8. The edges of the plume are clipped to values near 10^{-4} (mass fraction ~ 0.01). Note the mushroom shaped contours over the downwind section at 1500 m associated with the characteristic presence of plume buoyancy that produces an along-plume vortex pair. Comparisons of the predicted ground-level concentrations ($K_{ct} = C^*U_{ref}/Q_{source}$) for Case A to values predicted by the ISCST3 program for U_{ref} = 6.5, 7, & 8 m/sec are shown in Figure 9. For an elevated-plume release the ground-level concentrations are expected to rise from zero levels, reach a maximum and then decay with downwind distance. In this case the ground-level maxima occur downwind of the calculation domain. Wind velocities during the field experiment and the CFD simulations were observed to range between 6.5 to 8 m/sec over the height between 100 to 200 m above the ground through which the cloud rises over the first 1000 m downwind; hence, reference velocity used in the ISC3 model might range between 6.5 to 8 m/sec. The CFD results fall between the ISCST3 values, because ground-level values for this case are very low at the edge of the plume and quite sensitive to the assumed crosswind velocities. An additional comparison of the predicted plume centerline concentrations for Case A to values predicted by the ISCST3 program for U_{ref} = 8 m/sec is shown in Figure 10. As expected the centerline concentrations decay exponentially with downwind distance. Agreement is quite good, primarily because the ISCST3 model was designed to reliably predict plume behavior for plumes released over homogeneous terrain with modest building effects.

Predictions of DPM particle tracks are displayed in Figure 11, and contours of nodal and face values of mass deposition are shown in Figures 12 and 13.[5] Droplet deposition (mass/area/time) is calculated by the software

[5] In CFD nomenclature a "cell" is the discretized fluid volume over which the conservation equations are applied. A "wall cell" is a cell which adjoins a solid surface or boundary. A "face" is one of the side walls of the cell volume,

program as a specified cell face value at the center of each wall cell. This value is then used in the post-processing program to calculate nodal values between cells by interpolating between center faces. Since droplets accumulation is very sparse (often cells surrounding a target face may have no impacts), nodal values can be predicted to be significantly less than face values. Crosswind profiles of deposition were roughly distributed in a Gaussian manner over crosswind arcs which were less than those observed during the field measurements where wind veering occurred. Hence, to provide comparable values the CFD values were redistributed and averaged over the 30 degree arcs detected during the field experiment in a similar manner to that used by Hanna (1978). Calculated values are displayed in the following table, and the simple (3/3) satisfaction criteria suggested by Policastro et al. (1981a, 1981b) is noted next to each column: Y if predicted data falls within a 3 to 1/3 factor of observations, ~Y if it falls just slightly outside the factor and N if it fails to agree with the factor.

Table 2: Satisfaction Comparison Criteria Applied to Prediction of Average Arc Deposition

Deposition (kg/mo/km^2)	**CFD condition**	**X = 500 m**	**3/3 Criteria**	**X = 1000m**	**3/3 Criteria**
Field Observations	—	1080	--	330	--
Case A-1: Rosin-Rammler	Face values	758	Y	297	Y
	Nodal values	279	~Y	98	~Y
Case B-1: Rosin-Rammler	Face values	399	Y	148	Y
	Nodal values	299	~Y	79	N
Case B-2: Uniform Summed	Face values	2592	Y	467	Y
	Nodal values	984	Y	70	N
Case B-3: Rosin-Rammler	Face values	598	Y	296	Y
	Nodal values	299	~Y	98	~Y

The choice of inlet boundary-layer profile (Case A vs. B) did not change the (3/3) criteria agreement with observations; hence, one might conclude a simple inlet profile approach is adequate. The choice of particle distribution (Cases 1, 2, or 3) also did not change the (3/3) criteria agreement with observations; hence, the use of the standard Rosin-Rammler distribution without clipping smaller particles and allowing the software to integrate over different particle sizes is appropriate. Nodal averages tend to systematically underestimate deposition.

---

typically 6 for a hexagonal cell and 4 or 5 for a tetrahedral or pyramidal cell. “Nodes” are the corners of the cell, typically 8 for a hexagonal cell and 4 or 5 for a tetrahedral or pyramidal cell.

Finally, Figures 14 and 15 compare deposition magnitudes to observed, CFD, and analytic values predicted by ISCST-3 and Hanna (1978). Figure 14 displays arc-averaged depositions at the 500 and 1000 m measurement locations as a bar chart. The nodal averages are about one-half the face average values due to the interpolation errors discussed previously. One concludes the computations did reproduce the field measurements within acceptable limits. Indeed Case A-1 face values with the specified inlet profile and Rosin-Rammler representation of the Chalk Point source droplet distribution agreed within factors of 0.75 and 0.5 at 0.5 and 1.0 km, respectively. Even the worst case CFD comparisons at 0.5 and 1.0 km would be within a factor of 4. Figure 15 displays longitudinal variation of the observed, ISC3 and CFD Case A-1 deposition values. The ISC3 curve suggests maximum deposition occurred somewhere between 400 to 800 m downwind of the cooling tower.

4.0 CONCLUSIONS

The results of this study show that computational fluid dynamics (CFD) modeling can be expected to reproduce droplet deposition patterns downwind of cooling tower structures. The background review also noted significant limitations to the ISCST3 and SACTI analytic models when predicting near field dispersion and deposition of large particles in the vicinity of large up or downwind buildings. More specifically the literature review found that:

- Recommended analytic models (PAL2.1, ISCST3, & SACTI) that predict droplet deposition downwind of cooling towers do not account for the effects of building downwash and recirculation regions produced by large buildings immediately up or downwind of the source.
- In the ISCST3 model gravitational settling algorithms used assume relevant particle sizes are small (< 0.1 mm); hence, the model does not predict the behavior of large particles.
- Accurate estimation of the cooling tower source droplet distribution is necessary to produce reliable prediction of surface droplet deposition downwind. Incorrect distribution functions can result in deposition errors of 1 to 2 orders of magnitude in the near source region (< 500 m).
- Distributions for the cumulative mass fractions of various droplet sizes can be represented by the Rosin-Rammler type function. High efficiency drift eliminator systems result in Rosin-Rammler parameters of d_{mean} = 0.07-0.10 mm and shape factor n = 0.65-1.2; whereas low efficiency drift eliminator systems (or poorly installed or maintained high efficiency systems) results in Rosin-Rammler parameters of d_{mean} = 0.30-1.80 with n = 0.85-2.0.
- CFD has been used previously to estimate plume rise, plume visibility, plume touchdown, and air recirculation about cooling towers; however, no publication including CFD predictions of deposition were found.

The computational calculations and comparisons found that:

- The discrete particle model produced particle trajectories for releases in uniform low-turbulence flow fields over a range of particle sizes (0.001 to 2.0 mm) that duplicated published gravitational fall velocities (and by inference drag coefficients).
- The CFD program successfully predicted plume rise observed during the 1977 Chalk Point dye tracer experiment. Predicted values also fell close to the predictions of the Briggs plume rise formulae used by Hanna (1978).
- The CFD program successfully predicted droplet deposition observed during the 1977 Chalk Point dye tracer experiment well within the factor of 3 criteria proposed by Policastro et al. (1981a, 1981b). Predicted values were closer to the observed values than either the ISCST-3 or Hanna (1978) predictions.

ACKNOWLEDGEMENTS:

The author would like to acknowledge information and communications provided by Dr. D.J. Bergston, University of Saskatchewan; Dr. Richard Carhart, U. of Illinois at Chicago; Dr. Steven Hanna, Hanna Consultants; Dr. Raymond Hosker, NOAA; and Dr. Anthony Policastro, Argonne National Laboratory.

4.0 REFERENCES

AIAA 1998. *Guide for the Verification and Validation of Computational Fluid Dynamics Simulations*, AIAA G-077-1998e, (Co-authors, Conlisk, A.T. Jr., Oberkampf, W.L. and Sindir, M.), American Institute of Aeronautics and Astronautics, 1801 Alexander Bell Drive, Reston, VA 20191, 40 pp.

Anderson, John D., Jr. (1995), *Computational Fluid Dynamics: The Basics with Applications*, McGraw Hill, Inc., New York, 547 pp.

ASME (1975), Mathematical Models for Drift Transport, Chapter 6, *Cooling Tower Plume Modeling and Drift Measurement: A Review of the State of the Art*, American Society of Mechanical Engineering, Three Park Avenue, New York, NY 10016, pp. 64-76.

Banks, E., Meroney, R.N., Petersen, R.L. and Carter, J.J. (2003), Evaluation of Fluent for Predicting Concentrations on Buildings, *Proceedings of the Annual Meeting of the AWMA* (Air and Waste Management Association), San Diego, CA, June 2003, Paper No. 70223, 11pp.

Becker, B.R> and Burdick, L.F. (1994), Drift Eliminators and Fan System Performance, *1994 Cooling Tower Institute Annual Meeting*, Houston TX - February 13-16, 1994, 26 pp.

Bender, T.J., Bergstrom, D.J., and Rezkallah, K.S. (1996), A study on the effects of wind on the air intake flow rate of a cooling tower: Part 2. Wind wall study, *Journal of Wind Engineering and Industrial Aerodynamics*, Vol. 64, pp. 61-72.

Bender, T.J., Bergstrom, D.J., and Rezkallah, K.S. (1996b), A study on the effects of wind on the air intake flow rate of a cooling tower: Part 3. Numerical Study, *Journal of Wind Engineering and Industrial Aerodynamics*, Vol. 64, pp. 73-88.

Bergstrom, D.J., Derksen, D., and Rezkallah, K.S. (1993), Numerical study of wind flow over a cooling tower, *Journal of Wind Engineering and Industrial Aerodynamics*, Vols. 46 & 47, pp. 657-664.

Castro, I.P. (2003), CFD for External Aerodynamics in the Built Environment, *The QNET-CFD Network Newsletter,* Vol. 2, No. 2, pp 4-7. (See http://www.qnet-cfd.net/newsletter/6th/n6.html)

Castro, I.P. and Graham, J.M.R. 1999. Numerical Wind Engineering: The Way Ahead?, *Proc. Institute of Civil Engineers, Structures and Buildings*, Vol. 134, pp. 275-277. (See http://www.bmtfm.com/the_way_ahead.html)

Cermak, J.E., Davenport, A.G., Plate, E., and Viegas, D.X. (1995), *Wind Climate in Cities*, NATO Science Series, Series E, Applied Sciences No. 227, Kluwer Academic Publishers, Boston, 897 pp.

Chen, N.C.J. (1977), A Review of Cooling Tower Drift Deposition Models, Oak Ridge National Laboratory, Oak Ridge, TN, ORNL/TM-5357, 96 pp.

Chen, N.C.J. and Hanna, S.R. (1978), Drift Modeling and Monitoring Comparisons, *Atmospheric Environment*, Vol. 12., pp. 1725-1734. (also 1977 Cooling Tower Institute Annual Meeting, Houston, TX - January 31 to February 2, 1977 and Cooling Tower Institute Paper No. TP77-03).

Derksen, D.D., Bender, T.J., Bergstrom, D.J. and Rezkallah, K.S. (1996), A study on the effects of wind on the air intake flow rate of a cooling tower: Part 1. Wind Tunnel Study, *Journal of Wind Engineering and Industrial Aerodynamics*, Vol. 64, pp. 47-59.

England, W.G., Teuscher, L.H., and Taft, J.R. (1973), Cooling Tower Plumes - Defined and Traced by Means of Computer Simulation Models, *1973 Cooling Tower Institute Annual Meeting,* Houston TX - January 29-31, 1973, 41 pp.

Environmental Research and Technology, Inc. (1978), Assessment of atmospheric effects and drift deposition due to alternate cooling tower designs, Appendix D of *Air quality and climatic effects of the proposed Hat Creek project*, Document P-5074-F-D, Santa Barbara, CA, pp.B-1 to B-17, D4-1.

ERCOFTAC (2000), *The ERCOFTAC Best Practice Guidelines for Industrial Computational Fluid Dynamics* (Eds. Casey, M. and Wintergerste, T.), Ver. 1.0, *ERCOFTAC Special Interest Group on Quality and Trust in Industrial CFD*, ERCOFTAC Coordination Centre STI-LMF-EPFL, CH-1015, Lausanne, Switzerland, 95 pp.

Fluent 6.1 User's Guide (2003), Available on web by permission from Fluent at: http://www.fluentusers.com/fluent61/doc/doc_f.htm

Golay, M.W., Glantschnig, W.J., and Best, F.T. (1985), Comparison of Methods for Measurement of Cooling Tower Drift, *1985 Cooling Tower Institute Annual Meeting*, New Orleans, LA - January 21-23, 1985, Cooling Tower Institute Paper No. TP85-06, 61 pp.

Hangan, H.M. (2004), The C-FD-E concept. See internet website http://blow.blwtl.uso.ca/cfd/cfde.htm .

Hanna, S.R. (1978), A Simple Drift Deposition Model Applied to the Chalk Point Dye Tracer Experiment, *Environmental Effects of Cooling Tower Plumes, Symposium* on, May 2-4, 1978, U. of Maryland, PPSP CPCTP-22, WRRC Special Report No. 9, (Also NOAA, ATTDL Contribution File No. 78/3), pp. III-105 to III-118.

Hanna, S.R., Briggs, G.A., and Hosker, R.P. Jr. (1982), Cooling Tower Plumes and Drift Deposition, Chapter 11 of *Handbook on Atmospheric Diffusion*, U.S. Dept. of Energy, DOE/TIC-1123 (DE82002045), pp. 74-80.

Horst, T.W. (1983), A Correction to the Gaussian source-depletion model. *Precipitation Scavenging, Dry Deposition and Resuspension* (H.R. Pruppacher, R.G. Semonin, and W.G.N. Slinn, Eds.) pp. 1205-1218.

Huber, A.H. and Snyder, W.H. (1982), Wind tunnel investigation of the effects of a rectangular-shaped building on the dispersion of effluents from short adjacent stacks, *Atmos. Environ*., 176, pp. 2837-2848.

Jain, S.C. and Kennedy, J.F. (1978), Modeling Near-field Behavior of Mechanical Draft Cooling Tower Plumes, *Environmental Effects of Cooling Tower Plumes, Symposium* on, May 2-4, 1978, U. of Maryland, PPSP CPCTP-22, WRRC Special Report No. 9, pp. II-13 to II-30.

Jallouk, P.A., Kidd, G.J., Jr., and Shapiro, T. (1974), *Environmental Aspects of Cooling Tower Operation: Survey of the Emission, Transport, and deposition of Drift from the K-31 and K-33 Cooling Towers at ORGDP*, Union Carbide Corp., Oak Ridge, TN.

Kennedy, J.F. and Fordyce, H. (1974), Plume recirculation and interference in mechanical draft cooling towers,, *Cooling Tower Environment-1974, Symposium* at University of Maryland 4-6 March 1974, PPSP CPCTP-22, WRRC Special Report No. 9.

Lindahl, P.A. Jr. (2002), Wet Dry Cooling Towers for Plume Abatement and Water Conservation, *Dry cooling for Power Plants: Is this the future, Symposium on*, San Diego Chapter of Air and Waste Management Association, 31 May - 1 June, 2002, San Diego, CA. (See http://www.awmasandiego.org/SDC-2002/session4.htm)

McAlpine, J.D. and Ruby, M. (2004), Using CFD to Study Air Quality in Urban Microenvironments. Chapter 1 of *Environmental Sciences and Environmental Computing*. Vol. II (P. Zannetti, Editor), The EnvironComp Institute, pp. 1-31. (http://www.envirocomp.org)

Meroney, R.N., Leitl, B.M., Rafailidis, S., Schatzmann, M. and Pavegeau, M. (1999),Wind Tunnel and Numerical Modeling of Flow and Dispersion about Several Building Shapes, *Int. Workshop on ACFD for Wind Climate in Cities,* Hayama, Japan, August 24-26, 1998, *J. of Wind Engineering and Industrial Aerodynamics*, Vol 81 (1999), pp. 333-346.

Meroney, R.N., Letchford, C.W. and Sarkar, P.P. (2000), Comparison of Numerical and Wind Tunnel Simulation of Wind Loads on Smooth and Rough Domes Immersed in a Boundary Layer, *3rd Int. Symposium on Computational Wind Engineering*, Univ. of Birmingham, UK, 4-7 September 2000, 12 pp. (2002) *Wind and Structures*, Volume 5, No. 2

Meroney, R.N. and Chang, C.H. (2001), Numerical and Physical Modeling of Bluff Body Flow and Dispersion in Urban Street Canyons, *1st Americas Conference on Wind Engineering*, June 4-6, 2001, Clemson University, South Carolina, 7 pp. *J. Wind Eng. Ind. Aerodyn,.* Vol. 89, No. 14, pp. 1325ff.

Meroney, R.N., Neff, D.E. and Chang ,C.H. (2002a), Diagnosis of a Sick Building by the Wind Doctors *Proc. of the Second International Symposium on Advances in Wind & Structures (AWAS'02),* (C. K. Choi et. al. Editors) Pusan, Korea, August 21-23, 2002, pp. 43-52.

Meroney, R.N., Neff, D.E., Chang, C.H. and Predoto, R. (2002b), Computational Fluid Dynamics and Physical Model Comparisons of Wind Loads and Pedestrian Comfort Around a High Rise Building, Session on Computational Evaluation of Wind Effects on Buildings, *Proceedings of ASCE 2002 Structures Congress,* Denver, CO, April 4-6, 2002, 2 pp.

Moore, R.D., Wheeler, D.E., and Wilber, K.R. (1978), A comparison of Drift Transport Predictions for Various Types of Cooling Systems, *Environmental Effects of Cooling Tower Plumes, Symposium* on, May 2-4, 1978, U. of Maryland, PPSP CPCTP-22, WRRC Special Report No. 9,pp. III-231 to III-243.

Murakami, S. (1999), Past, present and future of CWE: the view from 1999. *Wind Engineering into the 21st Century*. (Ed. Larson, A., Larose, G.L. and Livesy, F.M.), Balkema Press, pp. 91-104.

NPARC Alliance (2004), Cfd Verification and Validation Web Site, NASA Glenn Research Center and Arnold

Engineering Development Center, USA., (See http://www.grc.nasa.gov/WWW/wind/valid/homepage.html).

Pasquill, F. (1962), Section 6.2 Deposition of Airborne Materials, *Atmospheric Diffusion: The Dispersion of Windborne Material from Industrial and Other Sources*, D. Van Nostrand Company, Ltd., London, pp. 226-239.

Petersen, R.L. (2004), ISC3 and PRIME Versus Wind Tunnel Observations for a Power Plant with Hyperbolic Cooling towers, *13th Conference on the Applications of Air Pollution Meteorology, Fifth Conference on Urban Environment,* Vancouver, BC 23-26 August 2004.

Petersen, W.B. and Rumsey, E.D. (1987), User's Guide for PAL 2.0- A Gaussian Plume Algorithm for Point, Area, and Line Sources, *EPA Publication No. EPA-600/8-87-009.* Office of Research and Development, Research Triangle Park, NC. (NTIS No. PB 87-168 787/AS), 23 pp.

Policastro, A.J. (2004), Private email communication, July 4, 2004.

Policastro, A.J., Dunn, W.E., Breig, M. and Ziebarth, J. (1978a), Comparison of Ten Drift Deposition Models to Field Data Acquired in the Chalk Point Dry Tracer Experiment, *Environmental Effects of Cooling Tower Plumes, Symposium* on (Supplement), May 2-4, 1978, U. of Maryland, pp. 76-84.

Policastro, A.J., Dunn, W.E., Breig, M. and Ratcliff, M. (1978b), Evaluation of Theory and Performance of Salt-Drift Deposition Models for Natural-Draft Cooling Towers, Environmental Effects of Atmospheric Heat/Moisture Release, Cooling Towers, Cooling Ponds, and Area Sources, *Proceedings. 2nd AIAA/ASME Thermophysics and Heat Transfer Conference*. Palo Alto, CA, May 24-26, 1978. Eds. K. Torrance and R.S. Watts pp. 2-3 to 2-14.

Policastro, A.J., Dunn, W.E., Berg, M.L. and Ziebarth, J.P. (1978c), The Chalk Point Dye Tracer Study: Validation of Models and Analysis of Field Data, *2nd Conference on Waste Heat Management and Utilization, Proceedings of*, Miami Beach, Florida, December 4-6, 1978. Eds. S.S. Lee and S. Sengupta, pp. 686-719.

Policastro, A.J., Dunn, W.E., Gavin, P, Boughton, B., and Ziebarth, J. (1981a), *Studies on Mathematical Models for Characterizing Plume and drift Behavior from Cooling Towers,, Volume 3: Mathematical Model for Single-Source(Single-Tower) Cooling Tower Drift Dispersion*, CS-1683, Volume 3, Research Project 906-2, Argonne National Laboratory, prepared for Electric Power Research Institute, Palo Alto, CA.

(See specifically Section 8: Performance of ANL Drift Model with Chalk Point Dye Study Data, pp. 8-1 to 8-9 of the above report.)

Policastro, A.J., Dunn, W.E., Breig, M. and Haake, K. (1981b), *Studies on Mathematical Models for Characterizing Plume and drift Behavior from Cooling Towers, Volume 5: Mathematical Model for Multiple Source (Multiple-Tower) Cooling Tower Drift Dispersion*, CS-1683, Volume 5, Research Project 906-1, Argonne National Laboratory, prepared for Electric Power Research Institute, Palo Alto, CA.

Power Generation Technologies (PGT) (2003), An Introduction to Cooling Tower Drift, *PGT-Power Generation Technologies Website* at http://www.pgt-online.com/services/driftbacground.shtml, 1 page.

QNET-CFD (2004), *Thematic Network on Quality and Trust for the industrial applications of Computational Fluid Dynamics (CFD).* European Union R&D program GROWTH, under contract number G1RT-CT-2000-05003, financed by the European Commission. (See http://www.qnet-cfd.net/ , Publishes the QNET-CFD Newsletter to enhance quality and trust issues at http://www.qnet-cfd.net/news.html)

Rao, K.S. (1981), Analytical Solutions of a Gradient-Transfer Model for Plume Deposition and Sedimentation, *NOAA Technical Memorandum ERL ARL-109,* 75 pp.

Rao, K.S. (1983), Plume Concentration Algorithms with Deposition, Sedimentation, and Chemical Transformation, *NOAA Technical Memorandum ERL ARL-124*, 87 pp.

Riddle, A., Carruthers, D., Sharpe, A., McHugh, C. and Stocker, J. (2004), Comparisons between FLUENT and ADMS for atmospheric dispersion modeling, *Atmos. Environ*., 38, pp. 1029-1038.

Ruby, M. and McAlpine, J.D. (2004), Estimating Odor Impact with Computational Fluid Dynamics, Proceedings WEF/A&WMA Odors and Air Emissions 2004, Water Environment Federation, Alexandria, VA, 25 pp. (see http://www.envirometrics.com).

Schatzmann, M. and Policastro, A.J. (1984), An Advanced Integral Model for Cooling Tower Plume Dispersion, *Atmospheric Environment*, Vol. 18, No. 4, pp. 663-674.

Schrecker, G.O. (1978), Variability of Drift Data and its Consequences to Calculated Drift Depositions, *Environmental Effects of Cooling Tower Plumes, Symposium* on (Supplement), May 2-4, 1978, U. of Maryland, pp. 54-75.

Scire, J.S. and Schulman, L.L. (1980), Modeling Plume Rise from Low-level Buoyant Line and Point Sources, *Proceedings Second Joint Conference on Applications of Air Pollution Meteorology*, 24-28 March, New Orleans, LA, pp. 133-139.

Schulman, L.L., Strimaitis, D.G. and Scire, J.S. (2000), Development and Evaluation of the PRIME Plume Rise and Building Downwash Model, *JAWMA,* Vol. 50, pp. 378-390.

Shin, S.H. and Meroney, R.N. (1989), Surface Pattern Comparability of Wind-tunnel Simulations of the Thorny Island dense Gas Dispersion Trials, Proceedings of 17th NATO/CCMS International Technical Meeting on Air Pollution Modelling and Its Application, 19-22 September 1988, Cambridge, (Editor (H. van Dop), *Air Pollution Modeling and Its Application VII*, Plenum Press, New York, 1989, pp. 77-88.

Shin, S.H., Meroney, R.N., and Williams, T. (1991), Wind Tunnel Validation for Vapor Dispersion from Vapor Detention System. *International Conference and Workshop on Modeling and Mitigating The consequences of Accidental Releases of Hazardous Materials*, New Orleans, LA, May 21-24, 1991.

Slater, J.W. (2004), Glossary and Tutorial, CFD Verification and Validation Website, NPARC Alliance, http://www.grc.nasa.gov/WWW/wind/valid/tutorial/glossary.html and http://www.grc.nasa.gov/WWW/wind/valid/tutorial/tutorial.html .

Stathopoulos, T. (1999), Computational wind engineering: past achievements and future challenges. *Journal of Wind Engineering and Industrial Aerodynamics*, Vol. 67/68, pp.509-532

Takata, K., Nasu, K., and Yoshikawa, H. (1996), Prediction of the Plume from a Cooling Tower, *1996 Cooling Tower Institute Annual Conference*, Houston, TX - February 1996, 27 pp.

U.S. EPA (1984), Cooling Towers, *Locating and Estimating Air Emissions from Sources of Chromium*, EPA-450/4-84-007g, pp. 174-181.

U.S. EPA (1989), Cooling Towers, Section 3.2 of Locating *and Estimating Air Emissions from Sources of Chromium (Supplement)*, EPA-450/2-89-002, pp. 23-39.

U.S. EPA (1995), *Document Number AP-42, Compilation of Air Pollution Emission Factors, Vol. 1 Stationary and Area Sources, Chapter13: Miscellaneous Sources, Section 13.4 Wet Cooling Towers*, 5th Edition, pp. 13.4-1 to 13.4-6. (www.epa.gov/ttn/chief/ap42/ch13/final/c13s04.pdf)

U.S. EPA (1995b), *User's Guide for the Industrial Source Complex (ISC3) Dispersion Models: Volume II - Description of Model Algorithms*, EPA-454/B-95-003b, pp. 1:5-1:30 and 1:35-1:46. (www.epa.gov/scram001/userg/regmod/isc3v2.pdf)

U.S. EPA (2003), CALPUFF, Guideline on Air Quality Models, *Appendix A of Appendix W to Part 51, 40 CFR, Chapter 1*, pp. 496-499. (www.epa.gov/scram001/tt22.htm#rec or www.src.com/calpuff/calpuff1.htm)

Van der Hoven, I. (1968), Deposition of Particles and Gases, *Meteorology and Atomic Energy 1968* (editor D. Slade), US. Atomic Energy Commission, pp. 202-207.

Webb, R.O., Wheeler, D.E., and Moore, R.D. (1978), Variations in the Chalk Point Cooling Tower Effluent Parameters and Their Effects on Drift Transport Modeling Results, *Cooling Tower Environment-1978, Proceedings of* a Symposium at the Center of Adult Education, University of Maryland (SUPPLEMENT), May 1978, pp. 42-53.

Wilber, K. and Vercauteren, K. (1986), Comprehensive Drift Measurements on a Circular Mechanical Draft Cooling Tower, *1986 Cooling Tower Institute Annual Meeting*, Houston, TX January 27-29, 1986, Cooling Tower Institute Paper NO. TP86-01, 33 pp.

Wistrom, G.K, and Ovard, J.C. (1973), Cooling Tower Drift Its Measurement, Control and Environmental Effects, *1973 Cooling Tower Institute Annual Meeting,* Houston, TX -January 29-31, 1973, Cooling Tower Institute Paper No. TP73-01, 26 pp.

FIGURE CAPTIONS:

1. Chalk Point Coal Fired Power Station (2640 MW), Maryland (Courtesy Power Plant Research Program, Department of Natural Resources, Maryland).
2. Droplet cumulative mass fraction distribution measured at the cooling tower exit during the Chalk Point Cooling Tower Dye Tracer Experiment, June 16-17, 1977.
3. Droplet cumulative particle distribution measured at the cooling tower exit during the Chalk Point Cooling Tower Dye Tracer Experiment, June 16-17, 1977.
4. Predicted and observed cooling tower plume centerline trajectory during the Chalk Point Dye Tracer Experiment, June 16-17, 1977.
5. CFD Case A predicted velocity profiles along domain centerline upwind and downwind of Chalk Point cooling tower.
6. CFD Case A predicted local turbulent intensity profiles along domain centerline upwind and downwind of Chalk point cooling tower.
7. CFD Case A predicted velocity profiles (x = -475, 100, 500, 1000, and 1500 m along centerline and 250 m to side) and isoconcentration surface (mass fraction ~ 0.01) for Chalk Point Dye Tracer Experiment.
8. CFD Case A predicted centerline water vapor isoconcentration contours: log (C^*U_{ref}/Q_{source}) (m^{-2}).
9. CFD predicted ground level concentration for Case A compared to ISCST-3 program predictions for U_{ref} = 6.5, 7, & 8 m/sec, $K_{ct} = C^*U_{ref}/Q_{source}$ (m^{-2}).
10. CFD predicted centerline plume concentrations for Case A compared to ISCST3 program predictions for U_{ref} = 8 m/sec, $K_{ct} = C^*U_{ref}/Q_{source}$ (m^{-2}).
11. CFD predicted particle track trajectories for Rosin-Rammler particle distribution at source (Case A-1, d_{mean} = 0.09 mm, n = 0.65).
12. CFD predicted deposition nodal contours (kg/m^2-sec) for Case A-1.
13. CFD predicted deposition face contours (kg/m^2-sec) for Case A-1.
14. Bar chart comparison of Chalk Point deposition data to CFD, ISCST-3 and Hanna (1978) predictions.
15. Deposition observed and predicted by CFD (Case A-1, Face), ISCST-3 and Hanna (1978).

Figure 1 Chalk Point Coal Fired Power Station (2640 MW), Maryland (Courtesy Power Plant Research Program, Department of Natural Resources, Maryland).

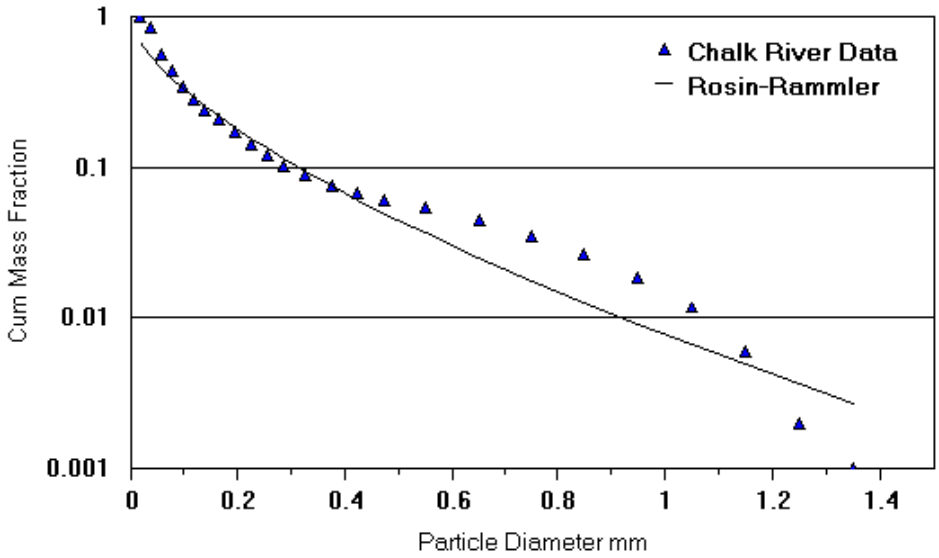

Figure 2 Droplet cumulative mass fraction distribution measured at the cooling tower exit during the Chalk Point Cooling Tower Dye Tracer Experiment, June 16-17, 1977.

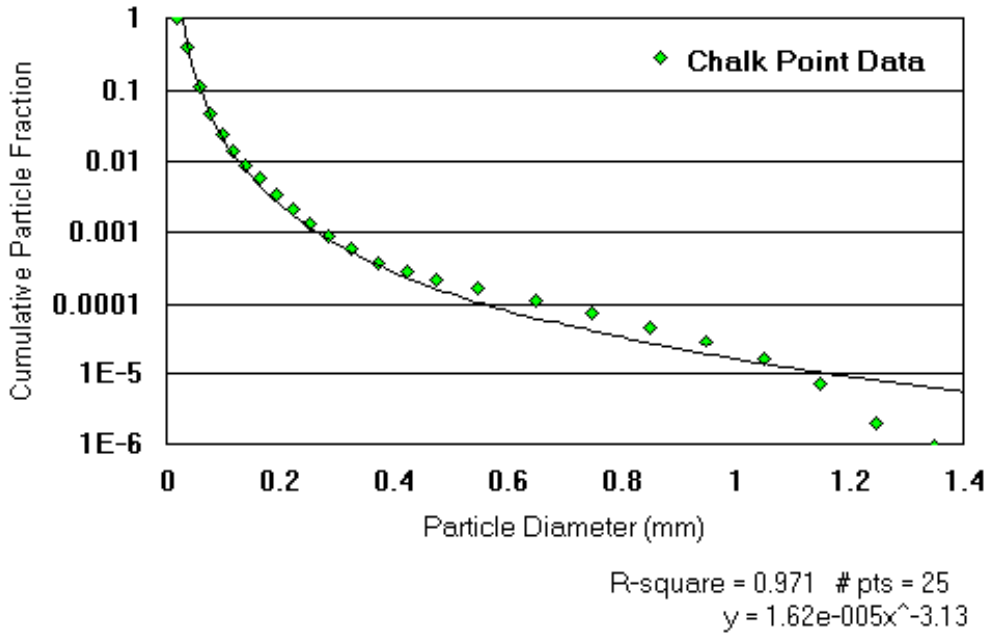

Figure 3 Droplet cumulative particle distribution measured at cooling tower exit during the Chalk Point Cooling Tower Dye Tracer Experiment, June 16-17, 1977. Best fit line equation and statistics noted.

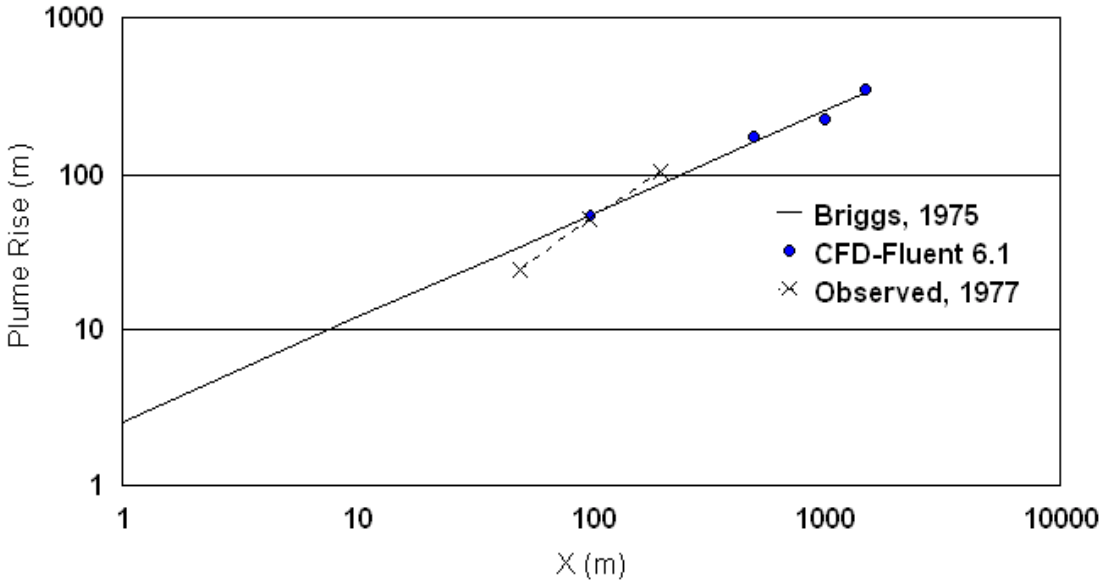

Figure 4 Predicted and observed cooling tower plume centerline trajectory for Case A during the Chalk Point Dye Tracer Experiment, June 16-17, 1977.

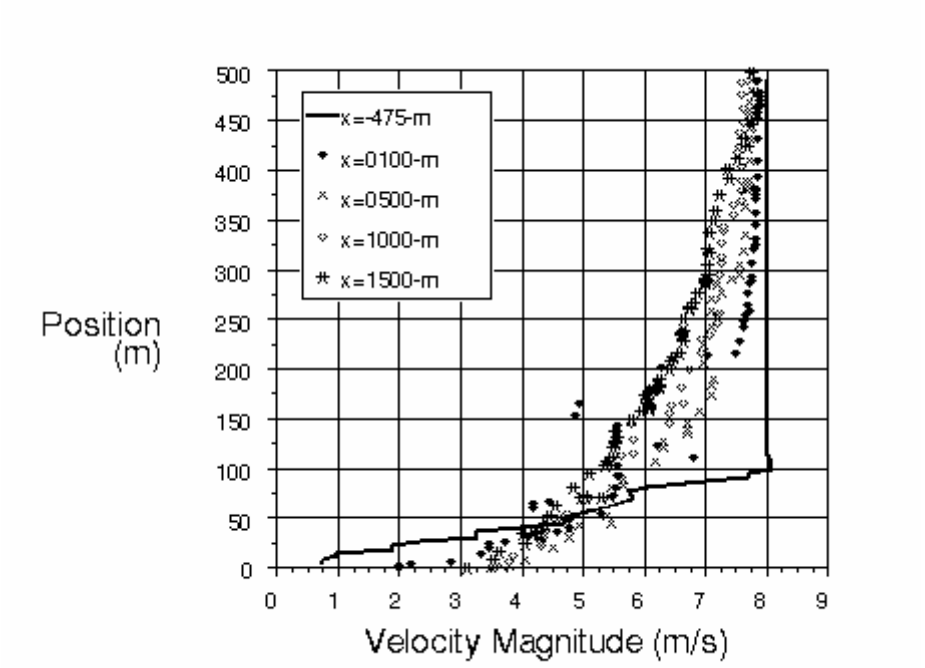

Figure 5 CFD predicted Case A velocity profiles along domain centerline upwind and downwind of Chalk Point cooling tower.

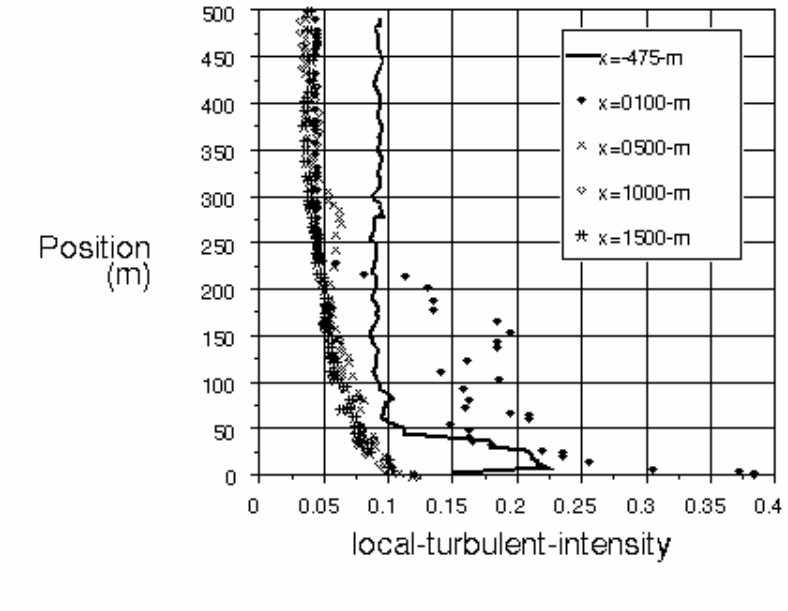

Figure 6 CFD predicted Case A local turbulent intensity profiles along domain centerline upwind and downwind of Chalk Point cooling tower.

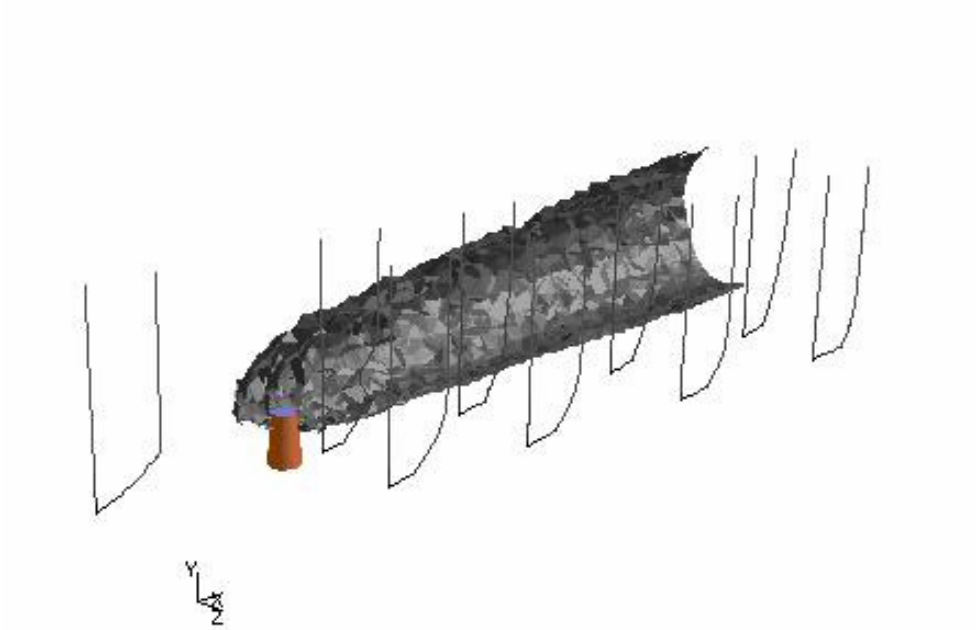

Figure 7 CFD predicted Case A velocity profiles (x = -475, 100, 500, 1000, and 1500 m along centerline and 250 m to side) and isoconcentration surface (mass fraction ~ 0.01) for Chalk Point Dye Tracer Experiment.

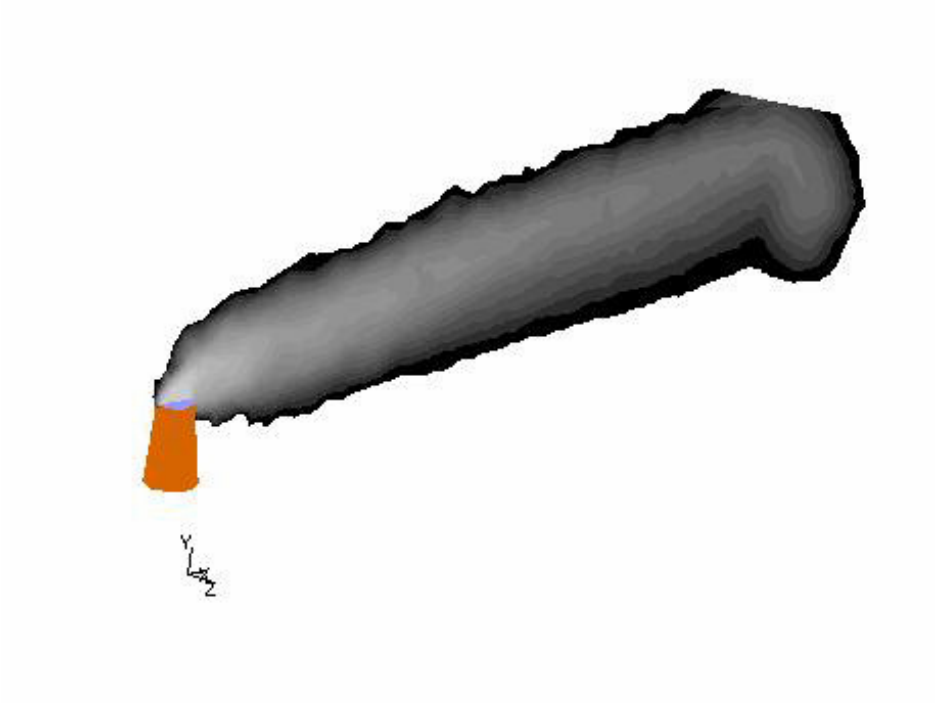

Figure 8 CFD predicted Case A centerline water vapor isoconcentration contours: log (C^*U_{ref}/Q_{source}) (m^{-2}).

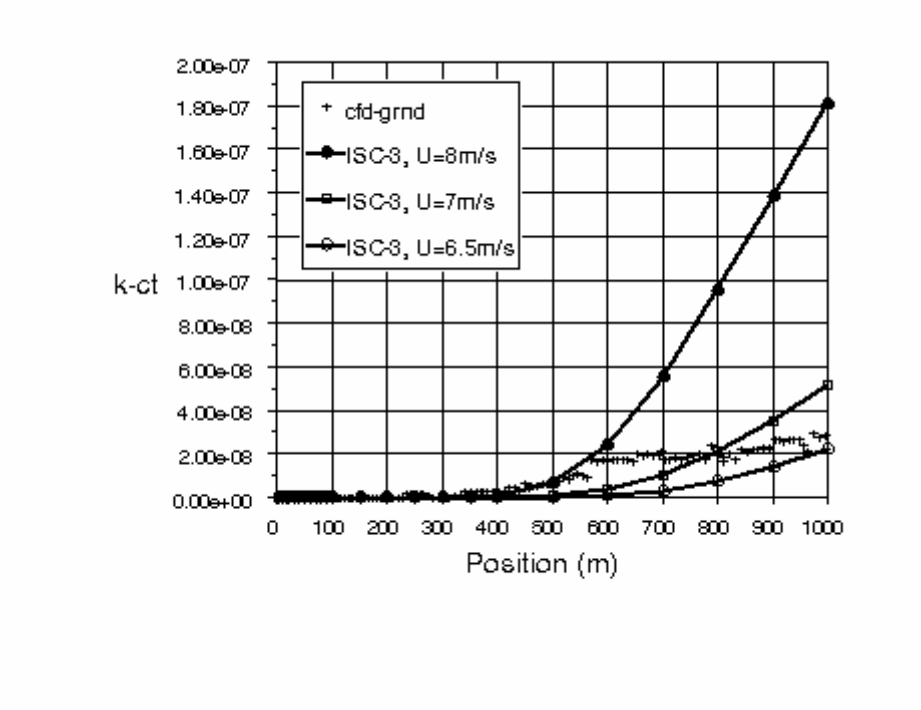

Figure 9 CFD predicted ground-level concentration for Case A compared to ISCST-3 program predictions for U_{ref} = 6.5, 7, & 8 m/sec, $K_{ct} = C*U_{ref}/Q_{source}$ (m^{-2}).

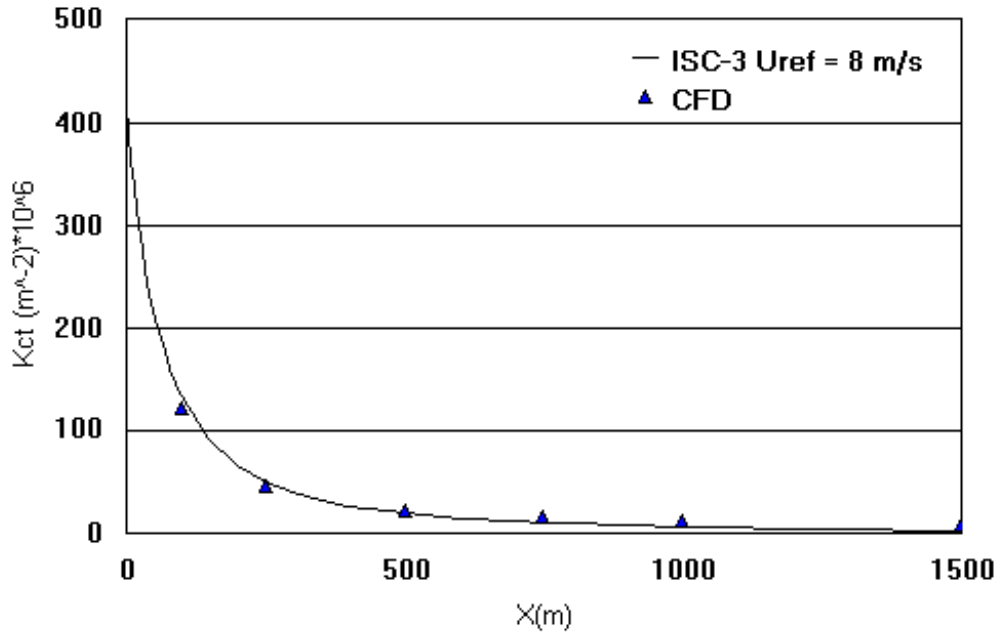

Figure 10 CFD predicted plume centerline concentration for Case A compared to ISCST-3 program prediction for U_{ref} = 8 m/sec, $K_{ct} = C*U_{ref}/Q_{source}$ (m^{-2}).

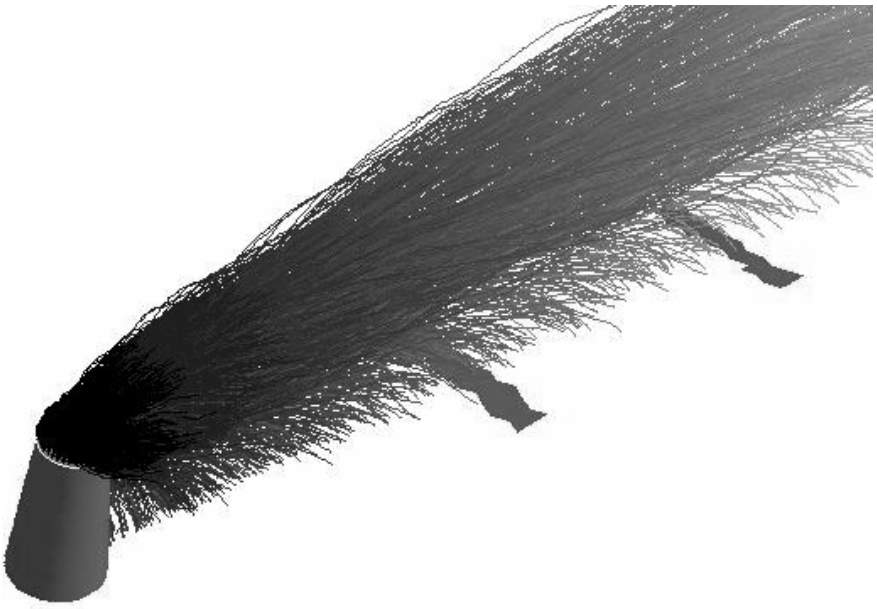

Figure 11 CFD predicted particle track trajectories for Rosin-Rammler particle distribution at source (Case A-1, d_{mean} = 0.09mm, n = 0.65).

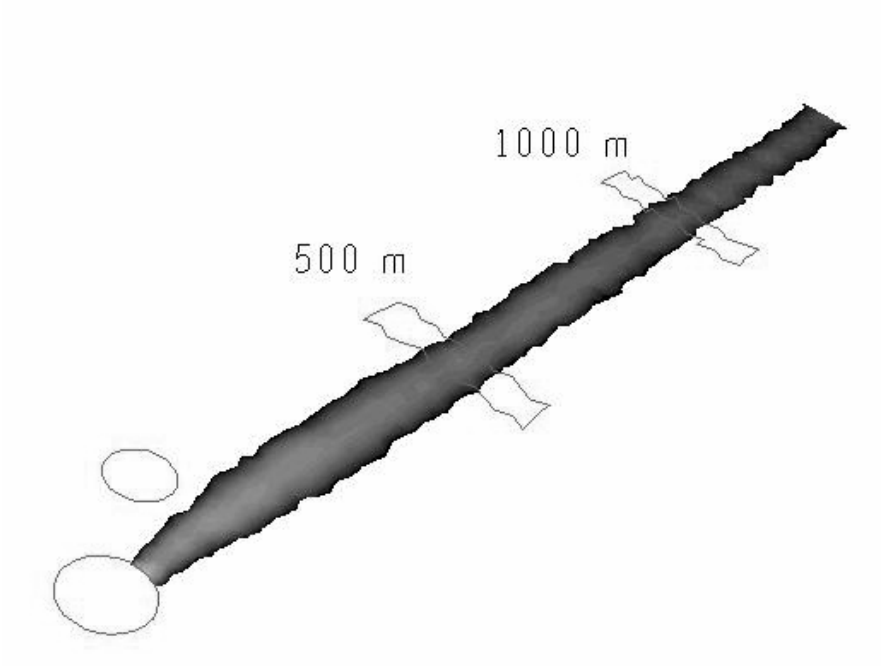

Figure 12 CFD predicted deposition nodal contours (kg/m^2 - sec) for Case A-1.

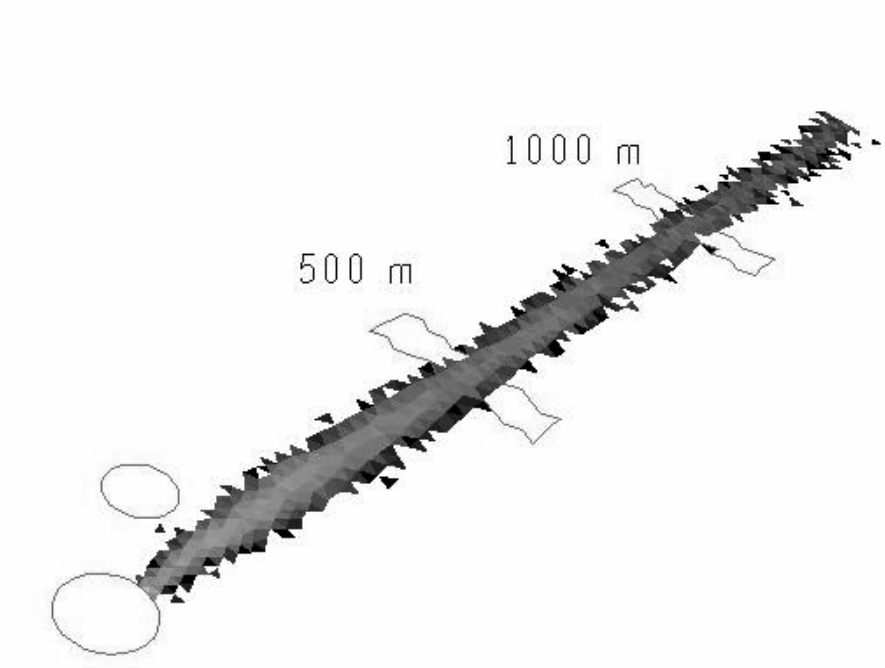

Figure 13 CFD produced deposition face contours (kg/m^2-sec) for Case A-1.

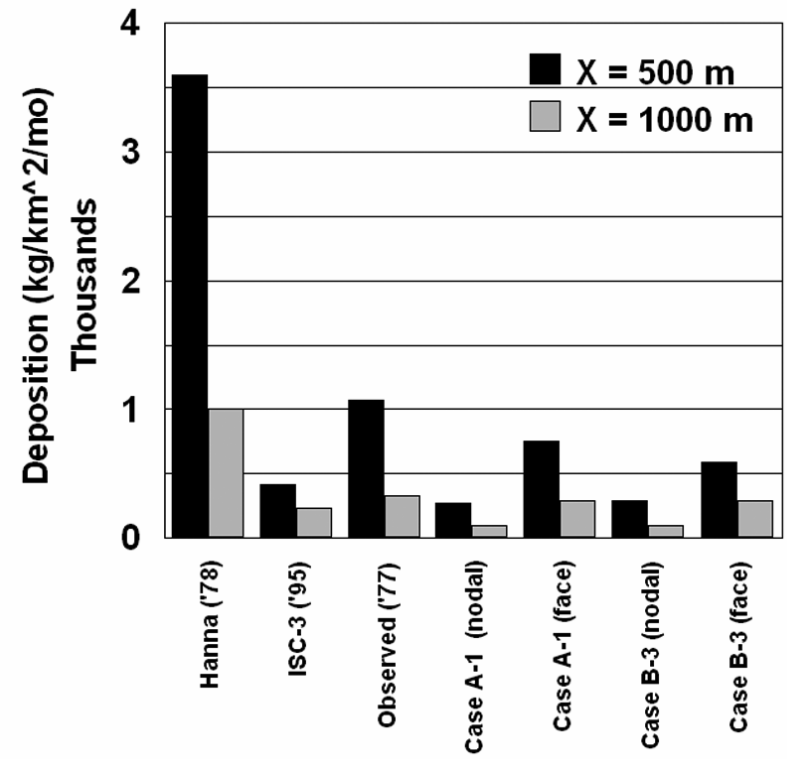

Figure 14 Bar chart comparison of Chalk Point deposition data to CFD, ISCST-3 and Hanna (1978) predictions.

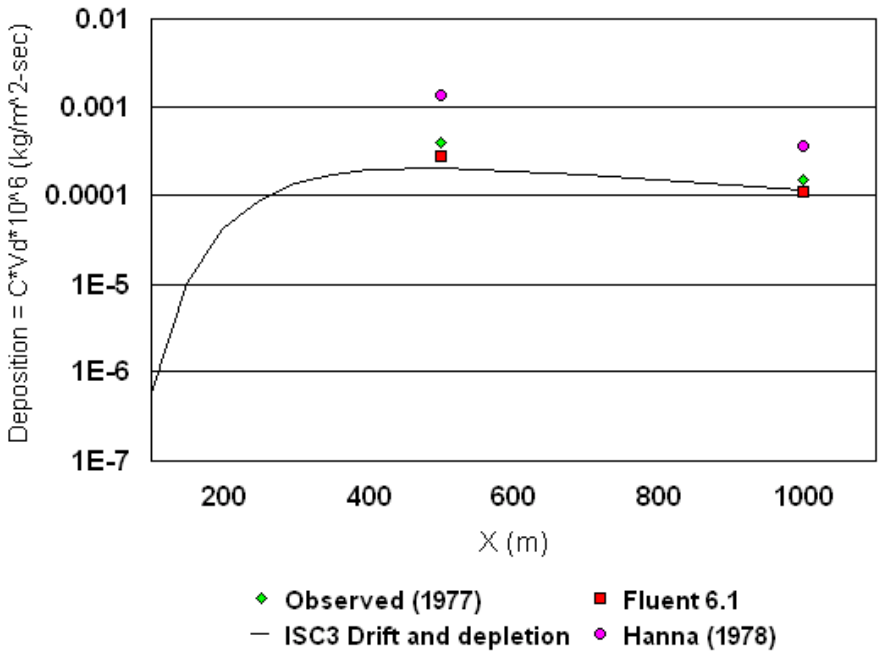

Figure 15 Deposition observed and predicted by CFD (Case A-1, Face), ISCST-3 and Hanna (1978).